11-1-1993

Numerical and Asymptotic Solutions for Peristaltic Motion of Nonlinear Viscous Flows with Elastic Free Boundaries

Dalin Tang
Worcester Polytechnic Institute, dtang@wpi.edu

Samuel Rankin

SIAM J. SCI. COMPUT.
Vol. 14, No. 6, pp. 1300–1319, November 1993

NUMERICAL AND ASYMPTOTIC SOLUTIONS FOR PERISTALTIC MOTION OF NONLINEAR VISCOUS FLOWS WITH ELASTIC FREE BOUNDARIES*

DALIN TANG† AND SAMUEL RANKIN†

Abstract. A mathematical model for peristaltic motion of nonlinear viscous flows with elastic free boundaries is introduced. An iterative numerical method is used to solve the free boundary problem. Long wave asymptotic expansion is developed and the zeroth order approximation is used as the numerical initial condition. The existence and uniqueness of the solution for the free boundary equation derived from the long wave expansion are proved. Computations were conducted to study the long wave approximation, the numerical solutions for the exact equations, and the influences of the parameters on the solutions.

Key words. peristaltic, Navier–Stokes, long wave, free boundary, elasticity

AMS subject classifications. 76, 39, 41, 34

1. Introduction. Peristaltic pumping, the physiological phenomenon of a circumferential progressive wave propagating along a flexible tube, plays an essential role in transporting fluid inside living organisms. Many modern mechanical devices have been designed on the principle of peristaltic pumping to transport fluids without internal moving parts, for example, the blood pump in the heart-lung machine and peristaltic transport of noxious fluid in the nuclear industry. Earlier mathematical work on the problem of peristaltic transport was based upon a viscous fluid model governed by the Navier–Stokes equations subject to a prescribed velocity on the boundary of the tube [11], [3]. A review of the research results can be found in the articles by Jaffrin and Shapiro [8] and Winet [21]. Numerical study of two-dimensional and axisymmetric peristaltic flows can be found in the articles by Takabatake, Ayukawa, and Mori [17], [18]. Recently, more refined models have been developed to deal with the peristaltic transport of a fluid-particle mixture or a heat-conducting fluid. The former was studied by Hung and Brown [7] and Kaimal [9], and the latter by Bestman [1] and Tang and Shen [19], [20].

In reality, the shape of the tube walls (e.g., blood vessels) is often unknown. They should be treated as free boundaries and solved as part of the solution. Experiments also suggest that the elastic properties of the tube walls should be taken into consideration [6], [10], [12]. In this paper, we introduce a three-dimensional (axisymmetric) model for viscous peristaltic motion with elastic free boundaries that combines three important factors: viscosity, elasticity, and free boundary. With the free boundary, this model should give a better representation of the actual physical situation than the fixed boundary models. Investigation of the free boundary model will provide useful information for designing equipment applying peristaltic motions and will lead to better understanding of some physiological processes involving peristalsis. However, the introduction of the free boundary makes this model difficult to solve. The fact that the domain is unknown makes it difficult to change the partial differential equation (PDE) system to a discretized difference system, which is the first step necessary to solve the PDE system using the finite difference method. To overcome this difficulty, we introduce a global iterative method for this model. The idea was originated from Fung [4]. To explain, we outline the method below.

Step 1. Obtain the long wave solution, which will be used as the numerical initial condition. The free boundary solution obtained from the long wave approximation will

*Received by the editors April 1, 1992; accepted for publication (in revised form) December 11, 1992. This research was supported in part by National Science Foundation grants DMS-9006043 and DMS-9209129.

†Mathematical Sciences Department, Worcester Polytechnic Institute, Worcester, Massachusetts 01609.

be used as the initial guess for the exact free boundary.

Step 2. With the boundary $\Gamma : r = H(x)$ obtained from Step 1 ($H(x)$ is the radius of the tube), use a local successive overrelaxation (SOR) method [20] to solve the system as a fixed boundary problem without the elasticity. The mapping

$$\xi = x, \tag{1.1}$$

$$\eta = r/H(x) \tag{1.2}$$

is used to map the (x, r) domain to a rectangular (ξ, η) domain. The number of iterations of the SOR method needed here should be determined by numerical experiment.

Step 3. Update the free boundary function $H(x)$ by using the elastic condition.

Step 4. With the newly updated $H(x)$, repeat Steps 2 and 3 until the desired accuracy is achieved. Adjust the number of local iterations if necessary to achieve the best convergence.

There are three key points in this method worth mentioning. (1) By using this procedure, the unknown domain becomes "known" at each global iteration and discretizing the PDE system becomes possible. (2) Using the long wave solution as the numerical initial condition is important to gain fast convergence. (3) The introduction of the mapping (1.1)–(1.2) makes the transformation of the (x, r) domain to a rectangular domain a fairly easy job.

In §2, we formulate the problem. The long wave asymptotic expansion is developed and solved in §3. The global iterative method is explained in §4. Results and discussions are given in §5.

2. Formulation. We consider viscous flow in an elastic tube while the shape of the tube is to be determined. A tension function is prescribed on the boundary to reflect the elastic property of the tube wall. The tube and the motion are assumed to be axisymmetric and the wave traveling along the tube (x-direction) is periodic. By choosing a coordinate system moving with the wave, the boundary becomes stationary. The problem is formulated in Fig. 1.

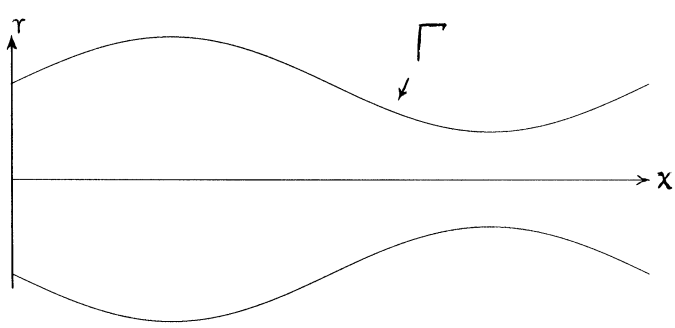

FIG. 1. *Peristaltic motion in an elastic tube.*

Equations of motion and continuity. Assuming the flow is Newtonian, viscous, and incompressible, we use the Navier–Stokes equations as the governing equations:

$$\rho \mathbf{u}_t + \rho(\mathbf{u} \cdot \nabla)\mathbf{u} = -\nabla p + \mu \nabla^2 \mathbf{u}, \quad \nabla \cdot \mathbf{u} = 0, \quad t \geq 0, x \in \Omega,$$

where ρ is the density, $\mathbf{u}$ the velocity with respect to the moving coordinate system, p the pressure, μ the dynamic viscosity, and Ω is the domain consisting of one period of the tube. In terms of cylindrical coordinates, the nondimensionalized equations of motion and continuity with axisymmetry are

$$\frac{\partial v_x}{\partial t} + v_x \frac{\partial v_x}{\partial x} + v_r \frac{\partial v_x}{\partial r} = -\frac{\partial p}{\partial x} + \frac{1}{R}\left(\frac{\partial^2 v_x}{\partial x^2} + \frac{1}{r}\frac{\partial v_x}{\partial r} + \frac{\partial^2 v_x}{\partial r^2}\right), \tag{2.1}$$

$$\frac{\partial v_r}{\partial t} + v_x \frac{\partial v_r}{\partial x} + v_r \frac{\partial v_r}{\partial r} = -\frac{\partial p}{\partial r} + \frac{1}{R}\left(\frac{\partial^2 v_r}{\partial x^2} + \frac{\partial^2 v_r}{\partial r^2} + \frac{1}{r}\frac{\partial v_r}{\partial r} - \frac{v_r}{r^2}\right), \tag{2.2}$$

$$\frac{\partial v_x}{\partial x} + \frac{v_r}{r} + \frac{\partial v_r}{\partial r} = 0, \tag{2.3}$$

where v_x and v_r are longitudinal and radial components of the velocity relative to the moving frame and R is the Reynolds number.

Free boundary. The free boundary $\Gamma : r = H(x)$ is to be determined as part of the solutions where $H(x)$ is the radius of the tube. We assume that $H(x)$ is periodic. Our result shows that for each prescribed initial opening

$$H(0) = H_0, \tag{2.4}$$

there is a solution to the free boundary equation obtained from the long wave approximation if certain conditions are met (see §3). This leads to the existence of the exact free boundary when the numerical method converges. However, the theoretical proof of the existence and uniqueness of the exact free boundary is a much harder problem and remains to be solved in the future.

Boundary conditions for the velocity and pressure. Considering boundary conditions, we assume no slipping between the fluid and wall, no penetration through the wall, and no horizontal motion of the wall. These lead to the following boundary conditions:

$$\mathbf{u}|_\Gamma = (v_x, v_r)|_\Gamma = (-C, f),$$

where Γ is the free boundary, C is the wave velocity, and f is determined by the radial motion of the free boundary. Recalling that the free boundary is $H = H(x) = H(x^* - Ct)$, where $H(x)$ is the radius of the free boundry and x^* is the old x-coordinate, we obtain

$$v_r|_\Gamma = \frac{dH}{dt} = \frac{\partial H}{\partial x^*}\frac{dx^*}{dt} + \frac{\partial H}{\partial t} = -CH'(x),$$

where the no-horizontal-motion condition $dx^*/dt = 0$ has been used. Now we have

$$\mathbf{u}|_\Gamma = (v_x, v_r)|_\Gamma = (-C, -CH'(x)). \tag{2.5}$$

It is easy to check that

$$\mathbf{u} \cdot \mathbf{n}|_\Gamma = 0,$$

i.e., the normal component of the velocity at the boundary is zero. Wave velocity C is prescribed with the tension function that is discussed below.

At $r = 0$, because of the symmetry, we assume

$$\frac{\partial v_x}{\partial r} = 0, \qquad v_r = 0.$$

At the two ends of the tube, we impose periodic conditions on the velocity and the pressure

$$v_x|_{x=0} = v_x|_{x=\ell'}, \tag{2.6}$$

$$v_r|_{x=0} = v_r|_{x=\ell'}, \tag{2.7}$$

$$p|_{x=0} = p|_{x=\ell'}, \tag{2.8}$$

where ℓ is the wave length. These periodic conditions are actually implied by the periodicity of the tension function and the Laplace law to be described below. Some numerical boundary conditions for the pressure at $r = 0$ and $\Gamma : r = H(x)$ will also be imposed. The details will be discussed later.

Additional boundary condition from elasticity—the Laplace law. Because the boundary is free, an additional boundary condition is needed to make the model complete. That condition comes from the consideration of the elastic property of the tube. Because of the complexity of structure of the tube walls in real application, there are many ways to introduce elasticity into a model. For simplicity, we will adopt the Laplace law to represent the elastic property of the wall [13]:

$$p|_\Gamma = \frac{T(x,r)}{r}, \tag{2.9}$$

where $T(x,r)$ is the prescribed tension function. Several cases are discussed in this paper. In practice, various functions can be introduced to find the best agreement with experimental data. When necessary, we may introduce more complicated elasticity laws involving stresses and strains of the walls, which would make the model more practical. The change of the elastic condition will affect only the part of updating the free boundary. Therefore, the numerical method will still be applicable with minor adjustments.

Remark. The prescribed tension is fundamental to the whole mechanism. We assume that it takes the form of a traveling wave

$$T = T(x^*, t, r) = T(x^* - Ct, r) = T(x, r),$$

with given wave speed C, period, and wave length. We are then looking for solutions in which the fluid velocity, pressure, and the free boundary also adopt the form of traveling waves with the same wave speed, period, and wave length as the imposed wave of elasticity.

From the Laplace law, it is clear that prescribing T is equivalent to prescribing the pressure at the free boundary.

Flux condition. Using $\mathbf{u} \cdot \mathbf{n}|_\Gamma = 0, \nabla \cdot \mathbf{u} = 0$, and the divergence theorem, we can prove [19]

$$\int_{A(x)} \mathbf{u} \cdot \mathbf{n} dA = \text{const} = Q,$$

where $A(x)$ is the cross section at x and Q is the flux. This is the so-called flux condition.

In terms of cylindrical coordinates, the flux condition can be written as

$$\int_{A(x)} \mathbf{u} \cdot \mathbf{n} dA = \int_0^{2\pi} \int_0^{H(x)} v_x \, r \, dr \, d\theta = Q$$

or

$$\int_0^{H(x)} v_x r dr = \frac{Q}{2\pi} = \text{const.} \tag{2.10}$$

For the fixed boundary model, it has been proved that for each prescribed flux, there exists a unique solution to the system [19]. A similar conclusion is also true for the fixed boundary model if we replace the flux condition by the pressure drop condition, i.e.,

$$p|_{x=\ell} - p|_{x=0} = \text{const} = P_d,$$

where P_d is the prescribed pressure drop. The relation between the flux and the pressure drop is almost linear for the fixed boundary model [20].

For the free boundary model, the situation is different. Due to the periodicity of the free boundary and the Laplace law just introduced, the pressure drop over one period of the tube must be zero. That means the pressure drop cannot be prescribed for the free boundary model. It is found in this paper that prescribing the flux is equivalent to prescribing the intial tube opening $H(0) = H_0$ for the free boundary model. For theoretical convenience, we choose to prescribe H_0.

Although we cannot prescribe the flux condition once H_0 is given, we still have that identity which will be used to derive the free boundary equation from the long wave approximation. The constant Q will be determined as part of the solution.

Remark. To prescribe pressure drop, tapering of the tube must be taken into consideration. This will be treated in a separate paper.

Remark. Recall that we are using a moving coordinate system. The laboratory longitudinal velocity u^* can be expresssed in terms of v_x by

$$u^* = v_x + C. \tag{2.11}$$

So the laboratory flux

$$Q^*(x^*) = \int_{A(x^*)} u^* dA = \int_{A(x^*)} v_x dA + \int_{A(x^*)} C dA = \text{const} + C \int_{A(x^*)} dA \tag{2.12}$$

will be a function of x^*, not a constant.

From the above, we have the mathematical model for the viscous flow with an elastic free boundary (in nondimensionalized version):

$$\begin{array}{ll}
\mathbf{u}_t + (\mathbf{u} \cdot \nabla)\mathbf{u} = -\nabla p + \frac{1}{R}\nabla^2 \mathbf{u}, & \text{(equation of motion)}, \\
\nabla \cdot \mathbf{u} = 0, & \text{(equation of continuity)}, \\
\mathbf{u}|_\Gamma = \left(-C, -C\frac{dH}{dx}\right), & \text{(boundary conditions for } \mathbf{u} \text{ at } \Gamma), \\
\frac{\partial v_x}{\partial r}|_{r=0} = 0, \qquad v_r|_{r=0} = 0, & \text{(boundary conditions for } \mathbf{u} \text{ at } r = 0), \\
\mathbf{u}|_{x=0} = \mathbf{u}|_{x=\ell}, & \text{(periodic condition for } \mathbf{u}), \\
p|_{x=0} = p|_{x=\ell}, & \text{(periodic condition for } p),
\end{array}$$

$$\Gamma : r = H(x), \qquad H(0) = H(\ell) = H_0, \text{ (conditions for the free boundary)},$$
$$p|\Gamma = \frac{T(x,r)}{r}, \qquad \text{(Laplace law)}.$$

Assuming axisymmetry, the stationary system can be expressed in terms of cylindrical coordinates as

$$v_x \frac{\partial v_x}{\partial x} + v_r \frac{\partial v_x}{\partial r} = -\frac{\partial p}{\partial x} + \frac{1}{R}\left(\frac{\partial^2 v_x}{\partial x^2} + \frac{1}{r}\frac{\partial v_x}{\partial r} + \frac{\partial^2 v_x}{\partial r^2}\right), \tag{2.13}$$

$$v_x \frac{\partial v_r}{\partial x} + v_r \frac{\partial v_r}{\partial r} = -\frac{\partial p}{\partial r} + \frac{1}{R}\left(\frac{\partial^2 v_r}{\partial x^2} + \frac{\partial^2 v_r}{\partial r^2} + \frac{1}{r}\frac{\partial v_r}{\partial r} - \frac{v_r}{r^2}\right), \tag{2.14}$$

$$\frac{\partial v_x}{\partial x} + \frac{v_r}{r} + \frac{\partial v_r}{\partial r} = 0, \tag{2.15}$$

$$(v_x, v_r)|_\Gamma = (-C, -CH'(x)), \tag{2.16}$$

$$\frac{\partial v_x}{\partial r}|_{r=0} = 0, \qquad v_r|_{r=0} = 0, \tag{2.17}$$

$$v_x|_{x=0} = v_x|_{x=\ell}, \qquad v_r|_{x=0} = v_r|_{x=\ell}, \tag{2.18}$$

$$p|_{x=0} = p|_{x=\ell}, \tag{2.19}$$

$$\Gamma : r = H(x), \quad H(0) = H(\ell) = H_0, \tag{2.20}$$

$$p|_\Gamma = \frac{T(x,r)}{r}, \qquad 0 \le x \le \ell, 0 < r \le H(x). \tag{2.21}$$

Compared with the fixed boundary model, this model treats the boundary as a free boundary. An additional boundary condition is introduced by using the Laplace law of elasticity. Instead of prescribing the flux condition, the initial opening of the tube $H_0 = H(0)$ is prescribed to ensure a unique solution of the system.

3. Long wave asymptotic approximation. Assume that $0 < d/\ell = \epsilon << 1$, where d is the average radius of the tube and ℓ is the wave length. Our previous experience indicates that $p = O(\epsilon^{-2})$. The Laplace law implies $T = O(p) = O(\epsilon^{-2})$. Then by assuming $R = O(\epsilon)$, the zeroth order long wave approximation will be essentially a one-dimensional linear system with free boundary; therefore, it is much easier to handle. Please note that although we made the assumption $R = O(\epsilon)$, it does not imply that our numerical method will be valid only for small Reynolds numbers since we are basically using this approximation as the numerical initial condition. The numerical method covered in §4 does apply to finite Reynolds number cases. For simplicity, when we simply replace, respectively, $x, \partial/\partial x, p, \ell, R, T$, by $x/\epsilon, \epsilon(\partial/\partial x), p\epsilon^{-2}, \ell/\epsilon, \epsilon R, T\epsilon^{-2}$ in (2.13)–(2.21), the system becomes

$$
\begin{aligned}
&\epsilon^2 v_x \frac{\partial v_x}{\partial x} + \epsilon v_r \frac{\partial v_r}{\partial r} = -\frac{\partial p}{\partial x} + \frac{1}{R}\left(\epsilon^2 \frac{\partial^2 v_x}{\partial x^2} + \frac{1}{r}\frac{\partial v_x}{\partial r} + \frac{\partial^2 v_x}{\partial r^2}\right),\\
&\epsilon^2 v_x \frac{\partial v_r}{\partial x} + \epsilon v_r \frac{\partial v_r}{\partial r} = -\epsilon^{-1}\frac{\partial p}{\partial r} + \frac{1}{R}\left(\epsilon^2 \frac{\partial^2 v_r}{\partial x^2} + \frac{\partial^2 v_r}{\partial z^2} + \frac{1}{r}\frac{\partial v_r}{\partial r} - \frac{v_r}{r^2}\right),\\
&\epsilon\frac{\partial v_x}{\partial x} + \frac{v_r}{r} + \frac{\partial v_r}{\partial r} = 0,\\
&(v_x, v_r)|_\Gamma = (-C, -C\epsilon H'(x)),\\
&\frac{\partial v_x}{\partial r}|_{r=0} = 0, \qquad v_r|_{r=0} = 0,\\
&v_x|_{x=0} = v_x|_{x=\ell}, \qquad v_r|_{x=0} = v_r|_{x=\ell},\\
&p|_{x=0} = p|_{x=\ell},\\
&\Gamma : r = H(x), \qquad H(0) = H(\ell) = H_0,\\
&p|_\Gamma = \frac{T(x,r)}{r}.
\end{aligned}
\tag{3.1}
$$

Because of the asymptotic assumptions, the odd terms of the asymptotic expansions of $\mathbf{u}, p$, and H will turn out to be zero. Therefore, we assume

$$
\begin{aligned}
\mathbf{u} &= \mathbf{u}_0 + \epsilon^2 \mathbf{u}_2 + \epsilon^4 \mathbf{u}_4 + \cdots,\\
p &= p_0 + \epsilon^2 p_2 + \epsilon^4 p_4 + \cdots,\\
H &= H_0 + \epsilon^2 H_2 + \epsilon^4 H_4 + \cdots,
\end{aligned}
$$

where $\mathbf{u}_i = (v_x^i, v_r^i)$. Substituting these into (3.1) for the zeroth order approximation, we obtain (in the following, we use H for $H_0(x)$ and H_0 for the initial opening),

$$\frac{1}{R}\left(\frac{1}{r}\frac{\partial v_x^0}{\partial r} + \frac{\partial^2 \partial v_x^0}{\partial r^2}\right) = \frac{\partial p_0}{\partial x}, \tag{3.2}$$

$$\frac{\partial p_0}{\partial r} = 0, \tag{3.3}$$

$$\frac{\partial v_r^0}{r} + \frac{\partial v_r^0}{\partial r} = 0, \tag{3.4}$$

$$(v_x^0, v_r^0)|_\Gamma = (-C, 0), \tag{3.5}$$

$$\frac{\partial v_x^0}{\partial r}|_{r=0} = 0, \qquad v_r^0|_{r=0} = 0, \tag{3.6}$$

$$v_x^0|_{x=0} = v_x^0|_{x=\ell}, \qquad v_r^0|_{x=0} = v_r^0|_{x=\ell}, \tag{3.7}$$

$$p_0|_{x=0} = p_0|_{x=\ell}, \tag{3.8}$$

$$\Gamma : r = H(x), \quad H(0) = H(\ell) = H_0, \tag{3.9}$$

$$p_0|_\Gamma = \frac{T(x,r)}{r}, \tag{3.10}$$

while

$$\int_0^H v_x^0 r dr = \frac{Q}{2\pi} \tag{3.11}$$

is an identity we will need in deriving the free boundary equation.

From (3.3), we see that $p_0 = p_0(x)$. Using (3.2) and the corresponding boundary conditions, we obtained

$$v_x^0 = \frac{1}{4}R(r^2 - H^2)\frac{\partial p_0}{\partial x} - C. \tag{3.12}$$

Plug into (3.11) and integrate

$$-\frac{R}{8}\frac{\partial p_0}{\partial x}H^4 - CH^2 = \frac{Q}{\pi}. \tag{3.13}$$

From (3.10), p_0 can be expressed in terms of $H(x)$ as

$$p_0 = \frac{T(x, H(x))}{H(x)}.$$

Thus (3.13) contains one unknown function $H(x)$ only. If $H(x)$ can be solved from (3.13) and (3.9), then p_0 and v_x^0 are also determined. It is easy to see from (3.4)–(3.6) that

$$v_r^0 = 0.$$

We consider the three cases below that are chosen because they are the three easiest simplifications of the general function $T(x, r)$. Comparison between the numerical and experimental results must be done to see how realistic these conditions are.

Case 1. $T(x, r) = T(r)$. From (3.10), $p_0 = (T(H))/(H) = p_0(H)$. Using this information and also letting $\ell = 1$ for simplicity, (3.13) and (3.9) become

$$-\frac{R}{8}\frac{\partial p_0}{\partial H}\frac{dH}{dx}H^4 - CH^2 = \frac{Q}{\pi}, \qquad H(0) = H(1) = H_0. \tag{3.14}$$

Equation (3.14) has a constant solution

$$H = \left(-\frac{Q}{(\pi C)}\right)^{1/2}. \tag{3.15}$$

It follows from here that

$$p_0 = \text{const}, \tag{3.16}$$

$$v_x^0 = -C, \tag{3.17}$$

$$v_r^0 = 0. \tag{3.18}$$

We also solved (3.14) numerically and (3.15) was the only solution we found. It turns out that (3.15)–(3.18) is also the exact solution to (2.13)–(2.21). Therefore, we suspect that the constant solution is the only solution to the system. However, we cannot yet provide a theoretical proof.

Case 2. $T(x,r) = T_0 b(x)$, where $b(x)$ is continuously differentiable and periodic with period $1, 0 < r_1 \leq b(x) \leq r_2 < \infty$. Now we have

$$p_0 = \frac{T_0 b(x)}{H}, \qquad p_{0x} = \frac{T_0 b'(x)H - T_0 b(x)H'}{H^2}.$$

The free boundary equation is

$$H'(x) = \frac{b'}{b}H + \frac{8}{RT_0}\left(\frac{C}{b(x)} + \frac{Q}{\pi b(x)H^2(x)}\right), \qquad H(0) = H(1) = H_0. \tag{3.19}$$

For (3.19), we have the following theorem.

THEOREM. *Let $b(x) \in C^1[0,1]$ be periodic with period 1, $b(0) = b(1) = 1$, $0 < b_1 \leq b(x) \leq b_2 < \infty$, $C \cdot Q \leq 0$, $\epsilon = (8/RT_0)$. Then for each $H_0 > 0$, there is $\epsilon_0 > 0$, such that for $\epsilon < \epsilon_0$, there exists a Q such that the free boundry equation* (3.19) *has a unique solution.*

Proof. We need the following lemma.

LEMMA ([2, Thm. 15.1, p. 148]). *Let* $\mathbf{X}$, $\mathbf{Y}$, $\mathbf{Z}$ *be Banach spaces, and let* $\mathbf{U} \subset \mathbf{X}$, *and* $\mathbf{V} \subset \mathbf{Y}$ *be neighborhoods of* x_0 *and* y_0, *respectively. Let* $\mathcal{F}(x,y) : \mathbf{U} \times \mathbf{V} \to \mathbf{Z}$ *be continuous and continuously differentiable with respect to* y. *Suppose also that* $\mathcal{F}(x_0, y_0) = 0$ *and* $\mathcal{F}_y^{-1}(x_0, y_0) \in \mathbf{L}(\mathbf{Z},\mathbf{Y})$. *Then there exist balls* $\overline{\mathbf{B}}_{\delta_x}(x_0) \subset \mathbf{U}$, $\overline{\mathbf{B}}_{\delta_y}(y_0) \subset \mathbf{V}$ *and exactly one map* $\mathcal{T} : \mathbf{B}_{\delta_x}(x_0) \to \bar{B}_{\delta_y}(y_0)$ *such that* $\mathcal{T}x_0 = y_0$ *and* $\mathcal{F}(x, \mathcal{T}x) = 0$ *on* $\mathbf{B}_{\delta_x}(x_0)$. *This map* $\mathcal{T}$ *is continuous.* $\square$

Proof of the theorem. Let $f(x) = 1/H(x)$, (3.16) is changed to

$$(bf)' = -\epsilon\left(Cf^2 + \frac{Q}{\pi}f^4\right).$$

Integrate from 0 to x,

$$b(x)f(x) = f(0) - \epsilon\int_0^x \left(Cf^2 + \frac{Q}{\pi}f^4\right)dx,$$

where $f(0) = 1/H(0)$. $f(0) = f(1)$ implies

$$Q = -\pi C\frac{\int_0^1 f^2 dx}{\int_0^1 f^4 dx}. \tag{3.20}$$

The equation now becomes a nonlinear integral equation

$$b(x)f(x) - f(0) + \epsilon C\int_0^x \left(f^2 - \frac{\int_0^1 f^2 dx}{\int_0^1 f^4 dx}f^4\right)dx = 0. \tag{3.21}$$

Introducing

$$g(x) = f(x) - \frac{f(0)}{b(x)}, \tag{3.22}$$

$$\mathcal{L}g = b(x)f(x) - f(0) = b(x)g(x), \tag{3.23}$$

$$
\begin{aligned}
\mathcal{N}g &= C\int_0^x \left(f^2 - \frac{\int_0^1 f^2dx}{\int_0^1 f^4dx} f^4\right) dx \\
&= C\int_0^x \left(\left(g(x)+\frac{1}{bH_0}\right)^2 - \frac{\int_0^1 \left(g+\frac{1}{bH_0}\right)^2 dx}{\int_0^1 \left(g+\frac{1}{bH_0}\right)^4 dx} \left(g+\frac{1}{bH_0}\right)^4 \right) dx, \qquad (3.24)\\
g \in \mathbf{Y} &= \{g | g(x) \in C[0,1], g(0)=g(1)=0\},
\end{aligned}
$$

then $\mathcal{L}: \mathbf{Y} \to \mathbf{Y}$ is one-to-one and onto, $\mathcal{L}^{-1}$ exists. Equation (3.20) becomes

$$\mathcal{L}g + \epsilon \mathcal{N}g = 0. \qquad (3.25)$$

Define

$$\mathcal{F}(\epsilon, g) = \mathcal{L}g + \epsilon\mathcal{N}g.$$

Then $\mathcal{F}$ is an operator from $\mathbf{R}\times\mathbf{Y}$ to $\mathbf{Y}$. It is easy to check that

$$\mathcal{F}(0,0)=0, \quad \mathcal{F}_g(0,0)=\mathcal{L}, \quad \mathcal{F}_g^{-1}(0,0)=\mathcal{L}^{-1}.$$

Then, by the lemma, there exist balls $\mathbf{B}_{\epsilon_0}(0) \subset R$, $\mathbf{B}_{\delta_y}(0) \subset \mathbf{Y}$, and a unique mapping $\mathcal{T}: \mathbf{B}_{\epsilon_0}(0) \to \mathbf{B}_{\delta_y}(0)$ such that

$$\mathcal{F}(\epsilon, \mathcal{T}\epsilon) = 0 \quad \text{for } \epsilon < \epsilon_0.$$

Furthermore, the mapping $\mathcal{T}$ is continuous, i.e., for δ small, we can choose ϵ such that

$$|\mathcal{T}_\epsilon| = |g(x)| \leq \delta.$$

We choose δ small so that

$$f(x) = g(x) + \frac{1}{b(x)H_0} \geq d_1 > 0.$$

Then

$$H(x) = \frac{1}{g(x)+\frac{1}{b(x)H_0}} = \frac{H_0 b(x)}{H_0 b(x) g(x) + 1} \qquad (3.26)$$

is the solution to the free boundary equation (3.19) and Q is given by (3.20). The proof is complete.

Case 3. $T(x,r) = T(r)b(x)$, where $b(x)$ is the same as in Case 2. For simplicity, let $T(r) = T_0 + T_1 r$. Similar calculation leads to

$$\frac{dH}{dx} = \frac{b'}{b}H + \frac{1}{T_0}\left(\frac{b'}{b}T_1H^2 + \frac{8C}{Rb} + \frac{8Q}{\pi RbH^2}\right). \qquad (3.27)$$

Equation (3.27) is similar to (3.19). By using the same procedure, similar results can be proved. We omitted the details here.

Remark. Although we have the existence and uniqueness of the free boundary for a long wave free boundary such as (3.19), we do not yet have the corresponding result for the exact system.

4. Numerical method for the exact system. The method is outlined in §2. As a numerical example, let $T = T_0(1 + a\sin 2\pi\alpha x)$, $0 \le x \le 1/\alpha$, where $\alpha = 1/\ell$ is the long wave parameter and ℓ is the wave length. Here we have assumed that the average radius of the tube $d = O(1)$ (Note: d is unknown.). The system to be solved is

$$
\begin{aligned}
&v_x\frac{\partial v_x}{\partial x} + v_r\frac{\partial v_x}{\partial r} = -\frac{\partial p}{\partial x} + \frac{1}{R}\left(\frac{\partial^2 v_x}{\partial x^2} + \frac{1}{r} - \frac{\partial v_x}{\partial r} + \frac{\partial^2 v_x}{\partial r^2}\right),\\
&v_x\frac{\partial v_r}{\partial x} + v_r\frac{\partial v_r}{\partial r} = -\frac{\partial p}{\partial r} + \frac{1}{R}\left(\frac{\partial^2 v_r}{\partial x^2} + \frac{\partial^2 v_r}{\partial r^2} + \frac{1}{r}\frac{\partial v_r}{\partial r} - \frac{v_r}{r^2}\right),\\
&\frac{\partial v_x}{\partial x} + \frac{v_r}{r} + \frac{\partial v_r}{\partial r} = 0.\\
&(v_x, v_r)|_\Gamma = (-C, -CH'(x)),\\
&\frac{\partial v_x}{\partial r}|_{r=0} = 0, \qquad v_r|_{r=0} = 0,\\
&\mathbf{u}|_{x=0} = \mathbf{u}|_{x=\ell},\\
&p|_{x=0} = p|_{x=\ell},\\
&\Gamma : r = H(x), \qquad H(0) = H(\ell) = H_0,\\
&p|_\Gamma = \frac{T_0(1 + a\sin 2\pi\alpha x)}{H}, \quad 0 < x < \ell, \quad 0 < r < H(x).
\end{aligned}
\tag{4.1}
$$

Step 1. Obtain the long wave approximation. In terms of the new parameters introduced during the long wave equation derivation, the free boundary equation is

$$
\frac{dH}{dx} = \left[(2\pi a\cos 2k\pi x)H + \frac{8Q}{\pi R T_0 H^2} + \frac{8C}{RT_0}\right] /[1 + a\sin 2\pi x], \tag{4.2}
$$

$$
H(0) = H(1) = H_0, \tag{4.3}
$$

where H_0 is the prescribed initial radius, C the wave velocity, and Q is to be determined with the solution. Equations (4.2)–(4.3) are solved numerically to get H_x. Back to the original parameters and variables (indicated by *), the pressure and velocity obtained from the long wave approximation are given by

$$
p_0^* = \frac{T_0^*(1 + a\sin 2\pi\alpha x^*)}{H}, \tag{4.4}
$$

$$
v_x^{0^*} = \frac{\alpha R^*}{4}(r^2 - H^2)\frac{T_0^* 2\pi a\cos 2\pi\alpha x^* H - T_0^*(1 + a\sin 2\pi\alpha x^*)dH/dx}{H^2} - C, \tag{4.5}
$$

$$
v_r^{0^*} = 0, \tag{4.6}
$$

where dH/dX is given by

$$
\frac{dH}{dx} = \left[(2\pi a\cos 2\pi\alpha x^*)H + \frac{8\alpha Q}{\pi R^* T_0^* H^2} + \frac{8C\alpha}{R^* T_0^*}\right] /[1 + a\sin 2\pi\alpha x^*]. \tag{4.7}
$$

Step 2. With the $H(x)$ obtained from Step 1, solve the fixed boundary problem on the domain $0 \leq x \leq 1/\alpha, 0 \leq r \leq H(x)$. Using (1.1)–(1.2), $\xi = x, \eta = r/H(x)$, we can transform the domain $0 \leq x \leq 1/\alpha$, $0 \leq r \leq H(x)$ to $0 \leq \xi \leq 1/\alpha$, $0 \leq \eta \leq 1$. In computing derivatives, the following formulas are useful:

$$\begin{aligned}
f_x &= f_\xi + f_\eta \eta_x, \\
f_r &= f_\eta \eta_r, \\
f_{xx} &= f_{\xi\xi} + 2f_{\xi\eta}\eta_x + f_{\eta\eta}\eta_x^2 + f_\eta \eta_{xx}, \\
f_{rr} &= f_{\eta\eta}\eta_r^2, \\
f_{xx} + f_{rr} &= f_{\xi\xi} + 2f_{\xi\eta}\eta_x + f_{\eta\eta}(\eta_x^2 + \eta_r^2) + f_\eta \eta_{xx},
\end{aligned} \tag{4.8}$$

where

$$\eta_x = -\frac{rH'(x)}{H^2}, \quad \eta_r = \frac{1}{H(x)}, \quad \eta_{xx} = -\frac{rHH'' - 2rH'^2}{H^3}.$$

Using the notation (u, v) for (v_x, v_r), the system in terms of (ξ, η) assumes the form

(4.9)

$$\begin{aligned}
u(u_\xi + u_\eta \eta_x) + v u_\eta \eta_r &= -(p_\xi + p_\eta \eta_x) \\
&\quad + \frac{1}{R}\left(u_{\xi\xi} + 2u_{\xi\eta}\eta_x + u_{\eta\eta}(\eta_x^2 + \eta_r^2) + u_\eta \eta_{xx} + \frac{1}{r} u_\eta \eta_r\right),
\end{aligned}$$

(4.10)

$$\begin{aligned}
u(v_\xi + v_\eta \eta_x) + v v_\eta \eta_r &= -p_\eta \eta_r \\
&\quad + \frac{1}{R}\left(v_{\xi\xi} + 2v_{\xi\eta}\eta_x + v_{\eta\eta}(\eta_x^2 + \eta_r^2) + v_\eta \eta_{xx} + \frac{1}{r} v_\eta \eta_r - \frac{v}{r^2}\right),
\end{aligned}$$

$$u_\xi + u_\eta \eta_x + \frac{v}{r} + v_\eta \eta_r = 0, \tag{4.11}$$

$$(u, v)|_\Gamma = \left(-C, -C\frac{dH}{d\xi}\right), \tag{4.12}$$

$$u_\eta|_{r=0} = 0, \qquad v|_{r=0} = 0, \tag{4.13}$$

$$u|_{x=0} = u|_{x=\ell}, \qquad v|_{x=0} = v|_{x=\ell}, \tag{4.14}$$

$$p|_{x=0} = p|_{x=\ell}, \tag{4.15}$$

$$\Gamma : \eta = 1, \qquad 0 \leq \xi \leq \frac{1}{\alpha}, \tag{4.16}$$

$$p|_\Gamma = \frac{T_0(1 + a \sin 2\pi\alpha\xi)}{H}, \tag{4.17}$$

where u, v, p, and the free boundary $H(x)$ are all periodic in ξ with period $1/\alpha$.

We use the regularized central difference scheme and the extended successive over-relaxation (ESOR) iterative method suggested by Strikwerda [14], [15] to solve this fixed boundary problem. The method has been used by the author successfully in [20] as it is relatively easy to program, is of second-order accuracy, and provides good convergence. The finite difference scheme used here is briefly explained below. Let d_1 and d_2 be the spans of finite differences for ξ, η, respectively. We use the following formulas for the derivatives to convert the differential equations into finite difference equations.

$$\begin{aligned}
f(i,j) &= f(\xi_i, \eta_j) = f(i \cdot d_1, j \cdot d_2). \\
f_{\xi\xi}(i,j) &= [f(i+1,j) + f(i-1,j) - 2f(i,j)]/d_1^2, \\
f_{\eta\eta}(i,j) &= [f(i,j+1) + f(i,j-1) - 2f(i,j)]/d_2^2, \\
f_{\xi\eta}(i,j) &= [f(i+1,j+1) - f(i-1,j+1) - f(i+1,j-1) + f(i-1,j-1)]/(4d_1d_2), \\
f_\xi(i,j) &= \delta_{\xi\circ}f - (1/6)d_1^2\delta_{\xi-}\delta_{\xi+}^2 f, \\
f_\eta(i,j) &= \delta_{\eta\circ}f - (1/6)d_2^2\delta_{\eta-}\delta_{\eta+}^2 f,
\end{aligned}$$

where

$$\begin{aligned}
(\delta_{\xi\circ}f)(i,j) &= [f(i+1,j) - f(i-1,j)]/(2d_1), \\
(\delta_{\xi+}f)(i,j) &= [f(i+1,j) - f(i,j)]/d_1, \\
(\delta_{\xi-}f)(i,j) &= [f(i,j) - f(i-1,j)]/d_1,
\end{aligned}$$

and the corresponding differences for η can be defined similarly. The third-order terms in the first difference formulas are necessary to have a regular scheme. The iterative scheme is given below:

(4.18)

$$\begin{aligned}
u^*(i,j) &= u(i,j) \\
&\quad -\omega \left\{ u(i,j) - \left[\frac{u(i+1,j) + u(i-1,j)}{d_1^2} + \frac{u(i,j+1) + u(i,j-1)}{d_2^2}(\eta^2 + \eta_r^2) \right.\right. \\
&\qquad + 2u_{\xi\eta}\eta_x + u_\eta\eta_{xx} - R(u(u_\xi + u_\eta\eta_x) + vu_\eta\eta_r) \\
&\qquad \left.\left. - R(p_\xi + p_\eta\eta_x) + u_\eta\eta_r/r \right] \Big/ \left[\frac{2}{d_1^2} + \frac{2}{d_2^2}(\eta_x^2 + \eta_r^2) \right] \right\},
\end{aligned}$$

(4.19)

$$\begin{aligned}
v^*(i,j) &= v(i,j) \\
&\quad -\omega \left\{ v(i,j) - \left[r^2 \left(\frac{v(i+1,j) + v(i-1,j)}{d_1^2} + \frac{v(i,j+1) + v(i,j-1)}{d_2^2}(\eta_x^2 + \eta_r^2) \right) \right.\right. \\
&\qquad \left. + r^2(2v_{\xi\eta}\eta_x + v_\eta\eta_{xx}) - Rr^2(u(v_\xi + v_\eta\eta_x) + vv_\eta\eta_r + p_\eta\eta_r) + rv_\eta\eta_r \right] \\
&\qquad \left. \Big/ \left[r^2 \left(\frac{2}{d_1^2} + \frac{2}{d_2^2}(\eta_x^2 + \eta_r^2) \right) + 1 \right] \right\},
\end{aligned}$$

$$p^*(i,j) = p(i,j) - \gamma\{r(u_\xi + u_\eta \eta_x) + v + r v_\eta \eta_r\}, \tag{4.20}$$

where u^*, v^*, and p^* are the updated values of the corresponding functions, and ω and γ are iteration constants. We used both finite differences and derivatives in (4.18)–(4.20) to shorten the formulas. When computing, those derivatives were calculated first and then (4.18)–(4.20) were performed.

We impose periodic boundary conditions on u, v, and p in ξ-direction. At $\eta = 0$, cubic interpolation was used for pressure, e.g.,

$$p(i,0) = 3(p(i,1) - p(i,2)) + p(i,3). \tag{4.21}$$

Cubic interpolation was also used for pressure at $\eta = 1$. Boundary condition (4.12) was used for (u, v) at $\eta = 1$. At $\eta = 0$, using second-order difference, (4.13) implies

$$u(i,0) = (4u(i,1) - u(i,2))/3, \tag{4.22}$$

$$v(i,0) = 0. \tag{4.23}$$

For computation, our experience indicates that $\omega = 0.001$—1.5 and $\gamma = 0.1\omega$ give good convergence. When the Reynolds number R is small, we chose $\omega = 1.5$, $\gamma = 0.1$. For larger $R (100 \leq R \leq 2000)$, we chose smaller ω and γ to make the algorithm converge.

Remark. The PDE needs two boundary conditions at $\eta = 0, 1$, and those conditions are given by (4.12)–(4.14). The cubic interpolations for the pressure at $\eta = 0, 1$ are numerical boundary conditions and do not make the system overdetermined. For reference on this regard, see [16, p. 298].

Step 3. We use the long wave approximation as the first guess. After a few local iterations for the fixed boundary problem, the boundary is updated according to (4.17):

$$H^*(\xi) = \frac{T_0(1 + a \sin 2\pi\alpha\xi)}{p(\xi, \eta)}\Big|_{\eta=1}.$$

Then the transformation (1.1)–(1.2) is modified using the new H^* and $\eta_x, \eta_r, \eta_{xx}$ are updated. This is one global iteration.

Step 4. Repeat Steps 2 and 3 as many times as needed. Our experience indicates that for most cases the number of local iterations is around 20. For some cases, we can achieve convergence by adjusting the number several times between 10 and 100 at the beginning stage of the computation.

Remark. "Convergence" is used here in the sense that the corrections to the numerical solutions made at each iteration, or, equivalently, the imbalances of the equations when the numerical solutions are plugged in will become and remain small after some iterations. (The imbalances are the L_2 norms of the parts inside $\{\cdots\}$ in (4.18)–(4.20). The relative imbalances are the above imbalances divided by the L_2 norms of u, v, and p, respectively.) The theoretical justification of the numerical method will be done in the future.

Computations were carried out for various situations and the results are given in §5.

5. Results of the computations and discussions. Since there are five parameters (α, R, T_0, a, H_0) and the solution contains the free boundary $H(x)$, velocity $(u, v) = v_x, v_r)$, pressure p, and flux Q, computations were carried out by changing each of the parameters, and solutions were observed to study the properties of the flow. We have made the following observations.

1. *Accuracy of the long wave approximation and numerical method.* From Table 1 we can see that the numerical method is roughly of second-order accuracy. The long wave and numerical solutions agree with each other very well (Tables 2 and 3).

2. *Influence of T_0 on the flow.* (i) Phase shift of the max–min of the free boundary. From Fig. 2 we see the phase shift of the max–min of the free boundary when T_0 is not large. However, when T_0 becomes large, the phase shift becomes small, and eventually becomes zero.

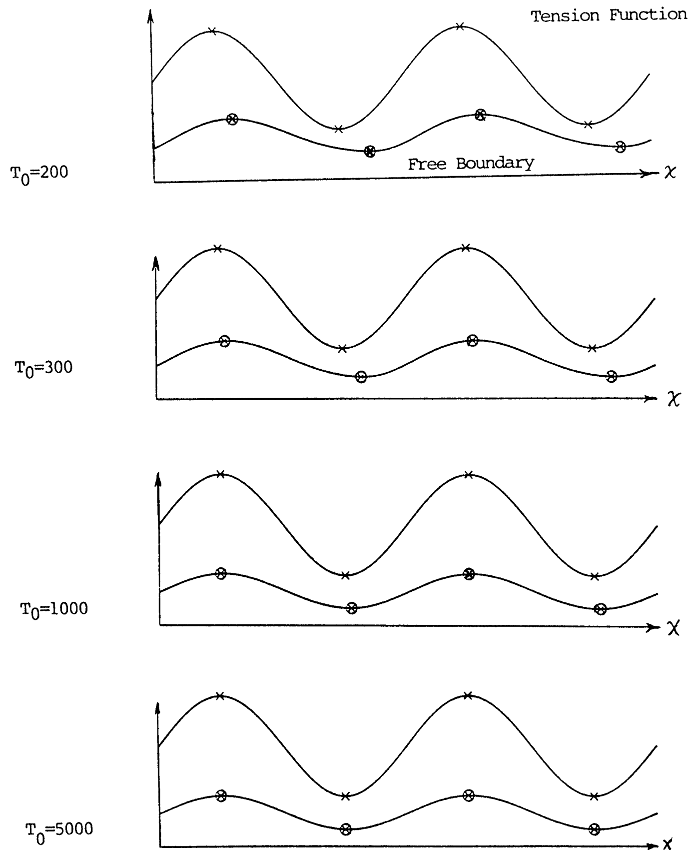

FIG. 2. *Free boundaries with T_0 changing.* $\alpha = 0.1$, $R = 0.1$, $H_0 = 0.5$, $a = 0.5$, $T_0 = 200$—5000.

(ii) Flow pattern. Our computation also indicates when T_0 becomes larger, the positive flow portion becomes larger and the tube becomes narrower.

(iii) $T_0 - Q$ curve. Figure 3 shows that the relation between T_0 and flux is not linear, and especially that the flux increases with T_0 very slowly when T_0 is greater than 2000.

(iv) Table 4 shows the max–min of the solutions with T_0 changing.

3. *Backflow and positive motion.* The v_x-minimum (negative) always appears at the narrower part of the tube, indicating that the fluid is leaking there. On the other hand, there are parts of "positive motion" at the wider part of the tube indicating the fluid is pushed forward by the wave. Usually the positive motion part is of a torus shape (note that the tube is axisymmetric).

4. *Pressure field.* Figure 4 gives the contour lines of the pressure fields. The picture shows the maximum of pressure appears at the right side of the "neck" and minimum

TABLE 1

Order of accuracy of the numerical method. $R = 0.2$, $T_0 = 250$, $a = 0.5$, $H_0 = 0.5$, $\ell = 5$, $d = 1$, $\alpha = 0.2$. *Numerical parameters:* $d_1 = \ell/m$, $d_2 = d/n$, $\omega = 1.5$, $\gamma = 0.1$, *local iteration* $= 20$, *main iteration* $= 200$.

		Imbalance of equations by the numerical solutions					
m	n	Eq. (2.1)	Eq. (2.2)	Eq. (2.3)	$\|u\|$	$\|v\|$	$\|p\|$
10	6	0.000099	0.000114	0.114018	2.288	0.390	147
20	12	0.000021	0.000023	0.037850	2.023	0.356	131
40	24	0.000009	0.000012	0.023615	1.962	0.341	126

Notes: (1) *Imbalance of an equation by the numerical solution is defined in the text.* (2) *Equations* (2.1) *and* (2.2) *are equations of motion;* (2.3) *is the equation of continuity.*

TABLE 2

Comparison between the long wave and numerical solutions. Re $= 1.0 \times \alpha$, $T_0 = 10/a^2$, $a = 0.5$, $H_0 = .5$, $C = 1.00$.

	Imbalance of equations			L_2-norms			
α	Eq. (2.1)	Eq. (2.2)	Eq. (2.3)	u	v	p	H
$a = 0.2$							
long	.00366	.00000	.62605	2.110	.000	127.8	1.402
exact	.00051	.00027	.03053	1.978	.342	122.9	1.416
$a = 0.1$							
long	.00248	.00000	.44182	2.976	.000	714.2	1.975
exact	.00013	.00038	.03014	2.925	.254	713.6	1.978
$a = 0.05$							
long	.00223	.00000	.31195	4.203	.000	4014.8	2.787
exact	.00002	.00007	.00888	4.182	.177	4014.9	2.789
$a = 0.025$							
long	.00218	.00000	.22039	5.940	.000	22638.1	3.938
exact	.00000	.00001	.00362	5.932	.124	22638.5	3.938
$a = 0.0125$							
long	.00217	.00000	.15576	8.398	.000	127852.7	5.566
exact	.00000	.00000	.00147	8.395	.088	127853.4	5.566
$a = 0.00625$							
long	.00217	.00000	.11011	11.874	.000	722654.9	7.870
exact	.00000	.00000	.00298	11.873	.061	722655.9	7.870
$a = 0.003125$							
long	.00217	.00000	.07785	16.791	.000	4086283.8	11.128
exact	.00000	.00000	.00543	16.791	.043	4086285.0	11.128

TABLE 3

Relative errors between long wave and numerical solutions. Re $= 1.0 \times \alpha$, $T_0 = 10/a^2$, $a = 0.5$, $H_0 = 0.5$, $C = 100$.

	L_2-norms of relative errors			L_2-norms of exact solutions			
α	$(u - u0)/u$	$(p - p_0)/p$	$(H - H0)/H$	u	v	p	H
.2	.08034	.108214	.011228	1.98	.342	122.9	1.4020
.10	.02422	.010197	.002264	2.93	.254	713.6	1.9749
.05	.00730	.002346	.000662	4.18	.177	4014.9	2.7873
.025	.00211	.000595	.000177	5.94	.126	22854.7	3.9498
.0125	.00051	.000143	.000043	8.39	.088	127853.4	5.5662
.00625	.00013	.000033	.000010	11.87	.061	722655.9	7.8698
.003125	.00003	.000007	.000002	16.79	.043	4086285.0	11.1281

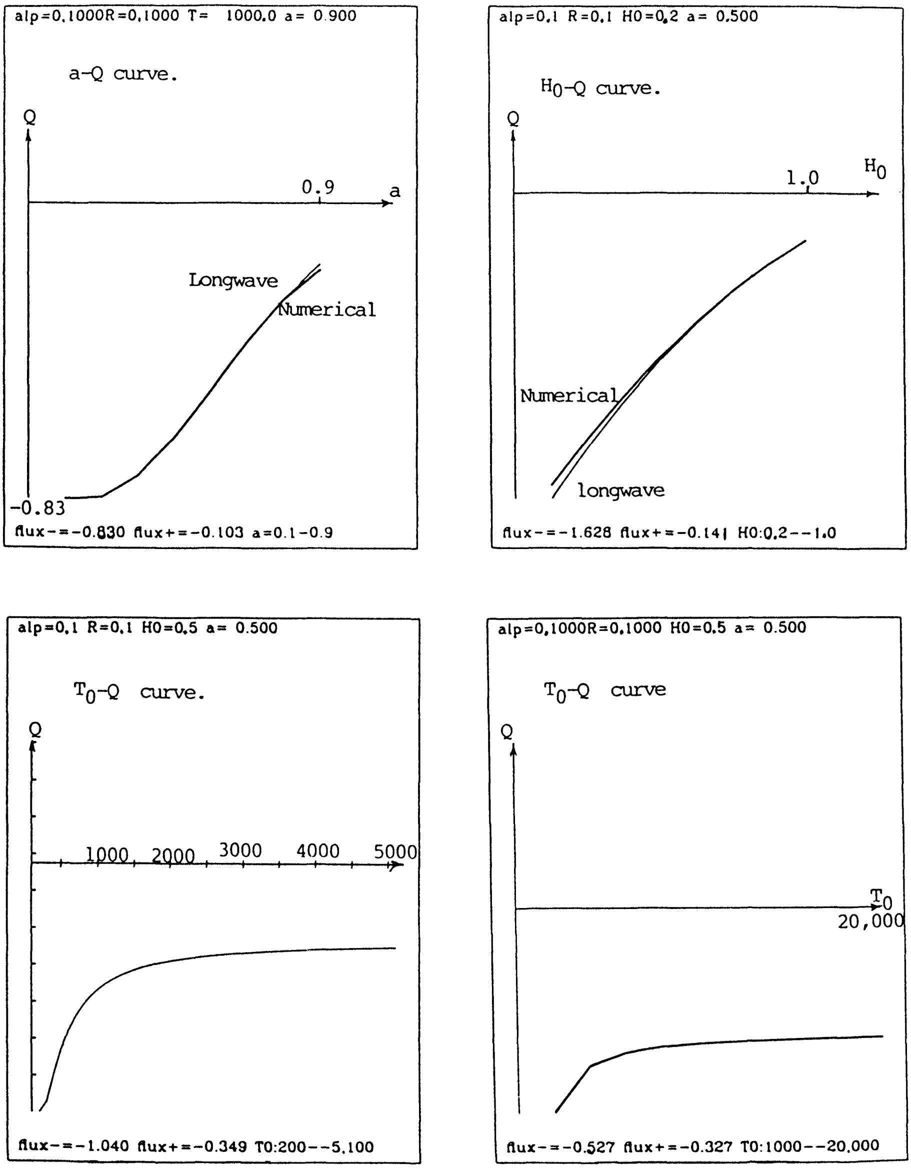

FIG. 3. *Relations between flux Q and other parameters.*

appears at the left side of the neck. So the pressure increases when passing the neck and decreases when going through the wider part of the tube. This agrees with the velocity pictures.

5. *Influence of Reynolds number on the flow.* Table 5 shows that the solution is not sensitive to the changes of Reynolds number when $0.001 \leq \text{Re} \leq 1000$ while $\text{Re}{\cdot}T_0 = 100$ is maintained. Numerically, smaller iterative parameters should be chosen to compute for large R values.

6. *Influence of a-change on the flow.* Figure 5 gives the velocity fields with respect

TABLE 4

Max–min *of solutions with* T_0 *changing.* $200 \le T_0 \le 1000$, $1000 \le T_0 \le 20{,}000$, $\alpha = 0.1$, $R = 0.1$, $a = 0.5$, $H_0 = 0.5$, $c = 1.0$.

T_0	$x$max–min		Hmin–max		Umin–Umax		Vmin–Vmax		Pmin–Pmax		flux
					Numerical solutions						
200	.400	.925	.493	.788	−1.69	0.65	−.113	0.89	179	469	−1.021
300	.350	.900	.468	.903	−1.87	.220	−.168	.128	278	628	−0.983
400	.325	.875	.437	.935	−1.97	.359	−.191	.145	395	806	−0.875
500	.325	.875	.407	.932	−2.03	.434	−.197	.152	529	1000	−0.774
600	.300	.850	.382	.920	−2.06	.481	−.198	.156	677	1201	−0.694
700	.300	.850	.363	.906	−2.09	.512	−.197	.158	833	1408	−0.633
800	.300	.850	.348	.892	−2.10	.534	−.195	.159	997	1614	−0.587
900	.300	.825	.337	.880	−2.12	.550	−.193	.159	1166	1825	−0.551
1000	.275	.825	.327	.870	−2.14	.564	−.191	.159	1340	2034	−0.522
2000	.275	.800	.283	.815	−2.19	.614	−.177	.159	3212	4094	−0.403
4000	.250	.775	.264	.783	−2.22	.625	−.167	.158	7143	8146	−0.356
6000	.250	.775	.259	.772	−2.21	.629	−.164	.157	11124	12163	−0.343
8000	.250	.775	.257	.767	−2.21	.630	−.162	.157	15116	16174	−0.337
10000	.250	.750	.256	.763	−2.22	.630	−.161	.157	19110	20180	−0.333
12000	.250	.750	.254	.761	−2.22	.631	−.160	.157	23106	24184	−0.331
14000	.250	.750	.254	.759	−2.22	.631	−.160	.157	27103	28187	−0.330
16000	.250	.750	.253	.758	−2.23	.631	−.159	.157	31101	32189	−0.328
18000	.250	.750	.253	.757	−2.23	.631	−.159	.157	35100	36190	−0.328
20000	.250	.750	.252	.757	−2.23	.631	−.159	.157	39098	40191	−0.327
					Long wave solutions						
200	.400	.950	.493	.798	−1.72	.041	.000	.000	177	462	−1.040
300	.350	.900	.466	.910	−1.92	.233	.000	.000	276	622	−0.997
400	.325	.875	.431	.934	−2.02	.357	.000	.000	396	803	−0.881
500	.325	.875	.401	.928	−2.08	.425	.000	.000	533	1000	−0.777
600	.300	.850	.377	.915	−2.12	.470	.000	.000	683	1202	−0.698
700	.300	.850	.359	.902	−2.15	.501	.000	.000	840	1409	−0.638
800	.300	.850	.345	.889	−2.16	.523	.000	.000	1004	1616	−0.592
900	.300	.825	.334	.877	−2.18	.540	.000	.000	1174	1826	−0.556
1000	.275	.825	.324	.867	−2.20	.553	.000	.000	1348	2034	−0.527
2000	.275	.800	.283	.814	−2.24	.609	.000	.000	3219	4092	−0.407
4000	.250	.775	.264	.782	−2.26	.628	.000	.000	7150	8141	−0.358
6000	.250	.775	.259	.772	−2.26	.633	.000	.000	11131	12157	−0.344
8000	.250	.750	.257	.766	−2.25	.634	.000	.000	15123	16168	−0.338
10000	.250	.750	.255	.763	−2.26	.635	.000	.000	19116	20174	−0.334
12000	.250	.750	.254	.761	−2.26	.635	.000	.000	23112	24178	−0.332
14000	.250	.750	.254	.759	−2.26	.636	.000	.000	27109	28180	−0.330
16000	.250	.750	.253	.758	−2.27	.636	.000	.000	31107	32183	−0.329
18000	.250	.750	.253	.757	−2.27	.636	.000	.000	35106	36184	−0.328
20000	.250	.750	.252	.757	−2.27	.646	.000	.000	39104	40185	−0.327

to the moving frame for $a = 0.2$ and 0.9. When a is small, there is no positive flow and no trapping. When a gradually increases, a small positive flow region appears near the center of the tube. When a becomes larger, the positive flow region becomes larger. a is the main parameter that has a major influence on flux, i.e., the efficiency of the fluid transport. The $a - Q$ curve is given in Fig. 3 for the a values between 0.1–0.9. The curves show that (i) when a is too small ($a \le 0.2$), the flux is not sensitive to a change for the simple reason that the wave is not deep enough to push the fluid forward. (ii) When a is greater than 0.3, the flux increases almost linearly with a.

TABLE 5

Max-min *of solutions with* R *changing,* $0.001 \leq \mathrm{Re} \leq 1000$. $\alpha = 0.1, R \cdot T_0 = 100, a = 0.3, H_0 = 0.5, C = 1.0$.

Numerical solutions											
R	$x$max–min		Hmin–max		Umin–Umax		Vmin–Vmax		Pmin	Pmax	Flux
0.001	.30	.825	.411	.719	−1.878	.040	−0.105	.090	155694	200000	−0.765
0.010	.30	.825	.411	.720	−1.872	.052	−0.105	.090	15557	20000	−0.765
0.100	.30	.825	.411	.719	−1.878	.040	−0.105	.090	1556	2000	−0.765
1.000	.30	.825	.411	.719	−1.877	.039	−0.105	.090	155	200	−0.765
10.000	.30	.825	.412	.722	−1.890	.050	−0.110	.094	15.4	20.0	−0.765
100.000	.30	.825	.411	.720	−1.902	.054	−0.104	.091	1.6	2.0	−0.765
1000.000	.30	.825	.411	.720	−1.902	.054	−0.104	.091	0.2	0.2	−0.765
Long wave solutions											
R	$x$max–min		Hmin–max		Umin–Umax		Vmin–Vmax		Pmin	Pmax	Flux
0.001	.30	.825	.410	.718	−1.901	.054	0.000	.000	156402	200000	−0.765
0.010	.30	.825	.410	.718	−1.901	.054	0.000	.000	15640	20000	−0.765
0.100	.30	.825	.410	.718	−1.901	.054	0.000	.000	1564	2000	−0.765
1.000	.30	.825	.410	.718	−1.901	.054	0.000	.000	156	200	−0.765
10.000	.30	.825	.410	.718	−1.901	.054	0.000	.000	15.6	20.0	−0.765
100.000	.30	.825	.410	.718	−1.901	.054	0.000	.000	1.6	2.0	−0.765
1000.000	.30	.825	.410	.718	−1.901	.054	0.000	.000	0.2	0.2	−0.765

Notes: Re *and* T_0 *are both changing while* $\mathrm{Re} \cdot T_0$ *remains constant. Smaller iterative parameters were used for greater* R *values.*

a=0.2

a=0.9

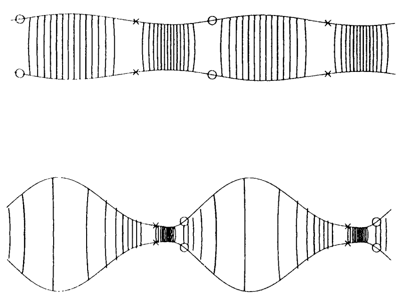

FIG. 4. *Pressure field with a changing.* $\alpha = 0.1$, $R = 0.1$, $H_0 = 0.5$, $T_0 = 1000$, $a = 0.2$—0.9.

a=0.2

a=0.9

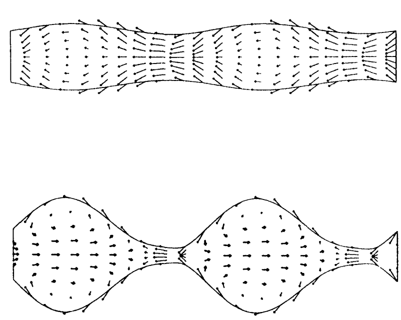

FIG. 5. *Velocity field of numerical solutions with a changing.* $\alpha = 0.1$, $R = 0.1$, $H_0 = 0.5$, $T_0 = 1000$, $a = 0.2$—0.9.

When drawing the velocity fields, the darker lines indicate forward motion while the lighter lines indicate backward motion. In the pressure field, circles indicate where the pressure is maximum and X indicates a minimum.

Acknowledgments. The authors wish to express their sincere appreciation to Professor C. S. Peskin and the referees for many helpful suggestions that improved the presentation of the paper.

REFERENCES

[1] A. R. BESTMAN, *Long wavelength peristaltic pumping in a heated tube at low Reynolds numbers*, Develop. in Mech., 10 (1979), pp. 195–199.

[2] K. DEIMLING, *Nonlinear Functional Analysis*, Springer-Verlag, New York, 1985.

[3] Y. C. FUNG AND C. S. YIH, *Peristaltic transport*, J. Appl. Mech., 37 (1968), pp. 901–905.

[4] Y. C. FUNG, *Biodynamics: Circulation*, Springer-Verlag, New York, 1984.

[5] ———, *Biomechanics: Motion, Flow, Stress, and Growth*, Springer-Verlag, New York, 1990.

[6] D. P. GIDDENS, C. K. ZARINS, AND S. GLAGOV, *Response of arteries to near-wall fluid dynamic behavior*, Appl. Mech. Rev., 43 (1990), pp. S98–S102.

[7] T. K. HUNG AND T. D. BROWN, *Solid particle motion in two dimensional peristaltic flows*, J. Fluid Mech., 73 (1976), pp. 77–96.

[8] M. Y. JAFFRIN AND A. H. SHAPIRO, *Peristaltic pumping*, Ann. Rev. Fluid Mech., 3 (1971), pp. 13–36.

[9] M. R. KAIMAL, *Peristaltic pumping of a Newtonian fluid with particles suspended in it at low Reynolds number under long wavelength approximations*, Trans. ASME, 45 (1978), pp. 32–36.

[10] D. N. KU, D. P. GIDDENS, C. K. ZARINS, AND S. GLAGOV, *Pulsatile flow and atherosclerosis in the human carotid bifurcation: positive correlation between plaque location and low and oscillating stress*, Arteriosclerosis, Vol. 5, May/June 1985.

[11] J. S. LEE, *The pressure-flow relationship in long-wave propagation in large arteries*, Proc. Symp. ASME Applied Mechanics Division, New York, 1966, pp. 96–120.

[12] B. B. LIEBER AND D. P. GIDDENS, *Post-stenotic core flow behavior in pulsatile flow and its effects on wall shear stress*, J. Biomechanics, 23 (1990), pp. 597–605.

[13] H. M. LIEBERSTEIN, *Mathematical Physiology*, Elsevier, New York, 1973.

[14] J. C. STRIKWERDA, *Finite difference methods for the Stokes and Navier–Stokes equations*, SIAM J. Sci. Statist. Comput., 5 (1984), pp. 56–58.

[15] J. C. STRIKWERDA AND Y. M. NAGEL, *A numerical method for the incompressible Navier–Stokes equations in three-dimensional cylindrical geometry*, J. Comput. Physics, 78 (1988), pp. 64–78.

[16] J. C. STRIKWERDA, B. A. WADE, AND K. P. BUBE, *Regularity estimates up to the boundary for elliptic systems of difference equations*, SIAM J. Numer. Anal., 27 (1990), pp. 292–322.

[17] S. TAKABATAKE AND K. AYUKAWA, *Numerical study of two-dimensional peristaltic flows*, J. Fluid Mech., 122 (1982), pp. 439–465.

[18] S. TAKABATAKE, K. AYUKAWA, AND A. MORI, *Peristaltic pumping in circular cylindrical tubes: A numerical study of fluid transport and it efficiency*, J. Fluid Mech., 193 (1988), pp. 267–283.

[19] D. TANG AND M. C. SHEN, *Peristaltic transport of a heat conducting fluid subject to Newton's cooling law at the boundary*, Internat. J. Engrg. Sci., 27 (1989), pp. 809–825.

[20] ———, *Numerical and asymptotic solutions for the peristaltic transport of a heat-conducting fluid*, ACTA Mechanica 83 (1990), pp. 93–102.

[21] H. WINET, *On the quantitative analysis of liquid flow in physiological tubes*, MRC Tech. Sum. Rep. No. 2456, University of Wisconsin–Madison, 1982.